Electronic Supplementary Material (ESI)

Ag-Au bimetallic nanocomposites stabilized with organic-inorganic composite polymer: synthesis and their regulated optical and catalytic properties

Lei Li, Rui Niu, Ying Zhang*

Key Laboratory of Applied Surface and Colloid Chemistry, Ministry of Education; School of Chemistry and Chemical Engineering, Shaanxi Normal University, Xi'an 710062, China

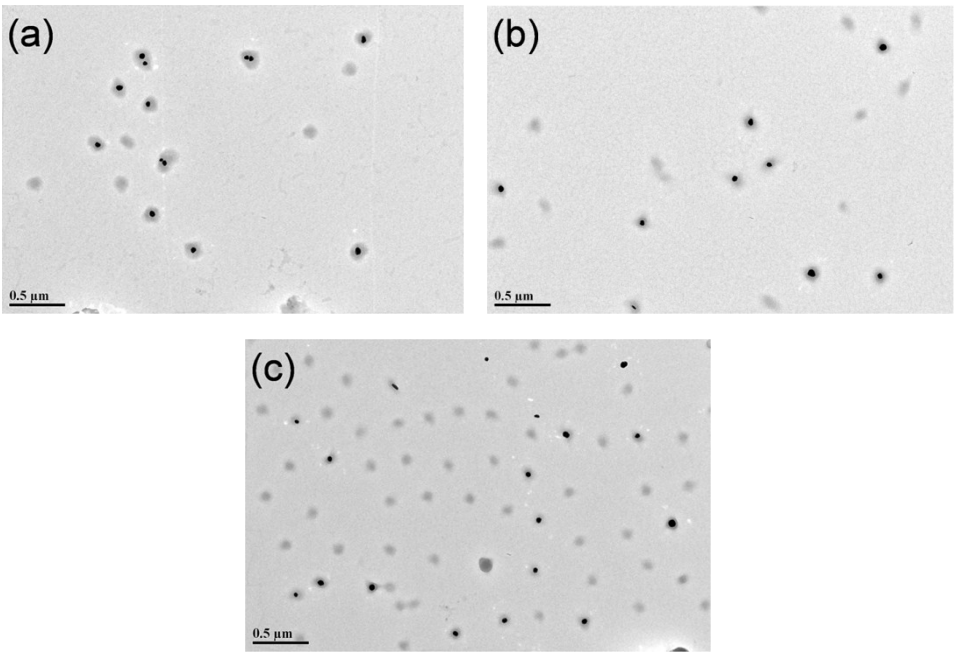

Fig. S1 TEM images of Ag@P(NIPAM-*co*-MAPTMS) hybrid microgels prepared with the different mass of NIPAM.
(a) 0.02 g, (b) 0.06 g, (c) 0.08 g

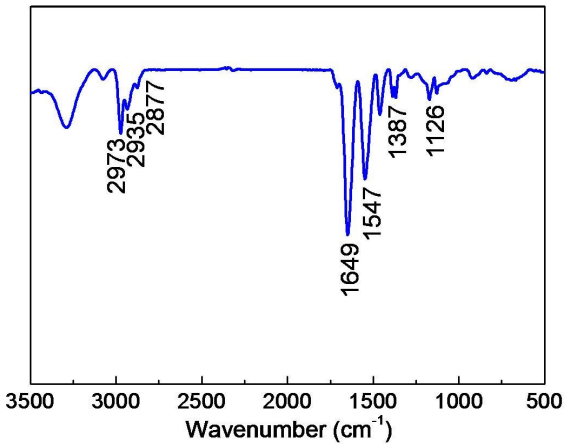

Fig. S2 FT-IR spectrum of Ag@P(NIPAM-*co*-MAPTMS) hybrid microgels.

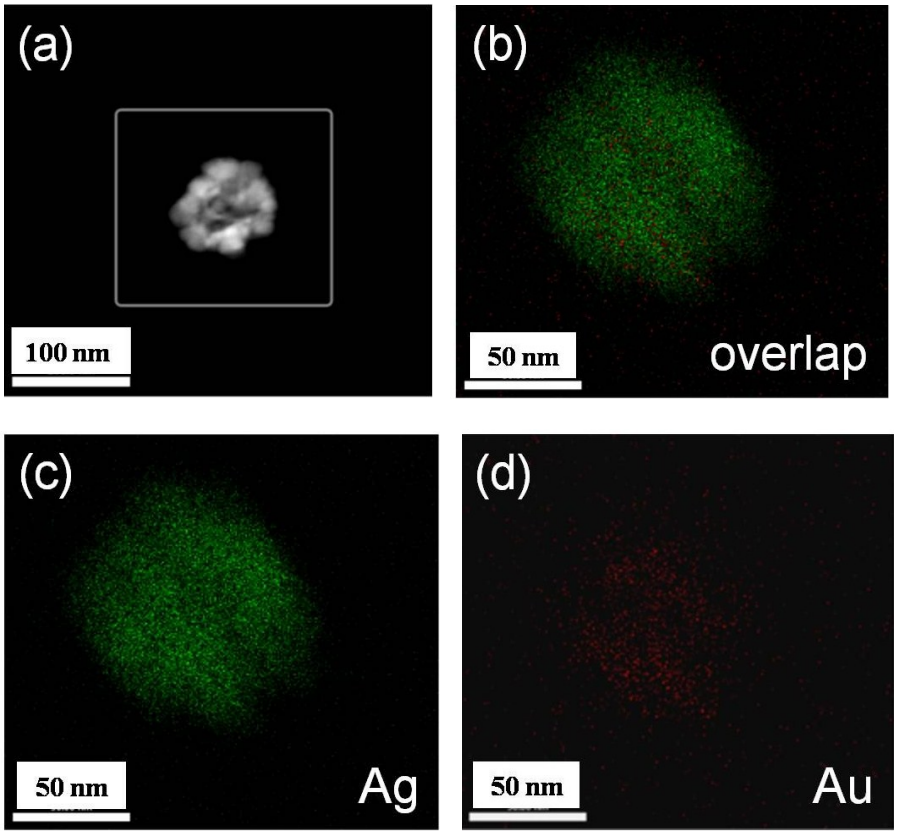

Fig. S3 STEM images for Ag-Au@P(NIPAM-*co*-MAPTMS)-2 hybrid microgels (a) and EDX mapping of Au and Ag elements (b-d).

Table S1 The electronic binding energies of Ag and Au for Ag-Au@P(NIPAM-*co*-MAPTMS) hybrid microgels from XPS results.

Samples	$V(HAuCl_4)$	Binding energy (eV)			
		Ag $3d_{5/2}$	Ag $3d_{3/2}$	Au $4f_{7/2}$	Au $4f_{5/2}$
Ag@P(NIPAM-*co*-MAPTMS)-2	3.0 mL	368.0	374.0	84.0	87.7
Ag@P(NIPAM-*co*-MAPTMS)-3	6.0 mL	367.7	373.7	83.7	87.4
Ag@P(NIPAM-*co*-MAPTMS)-4	9.0 mL	367.5	373.5	83.5	87.2

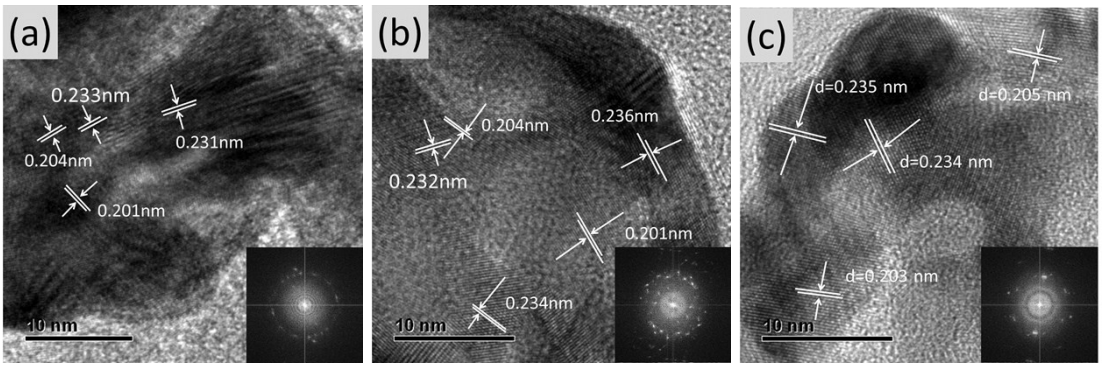

Fig. S4 HR-TEM and the FFT images (inset) of the Ag-Au@P(NIPAM-*co*-MAPTMS) bimetallic hybrid microgels at different volume of $HAuCl_4$.

(a) 3.0 mL, (b) 6.0 mL, (c) 9.0 mL

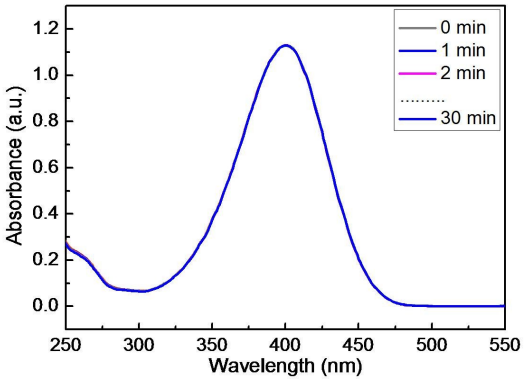

Fig. S5 UV-Vis absorption spectra for 4-NP in the absence of catalyst.

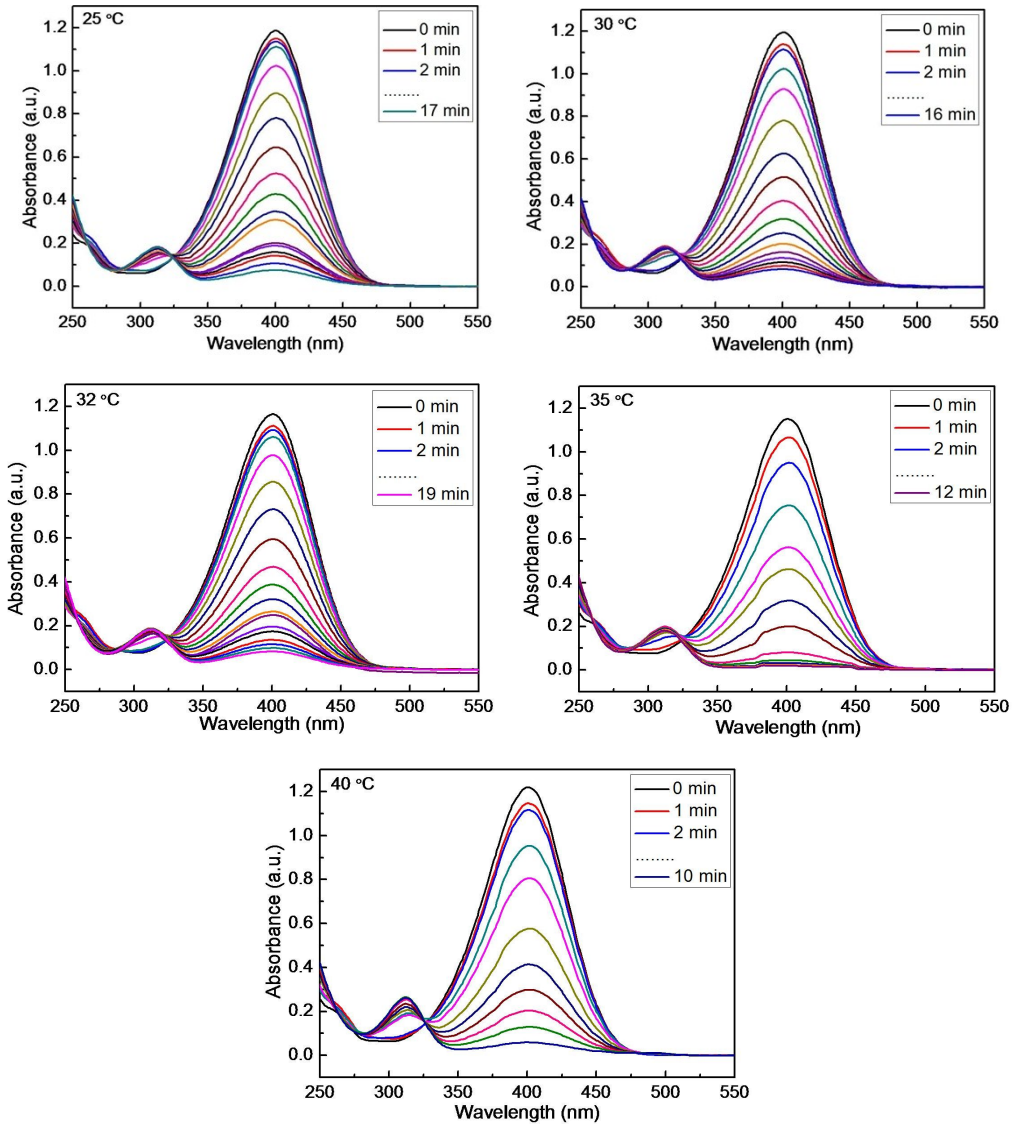

Fig. S6 UV-Vis absorption spectra for the reduction of 4-NP in the presence of Ag-Au@P(NIPAM-*co*-MAPTMS)-3 hybrid microgels under different temperature.

Table S2 The activation parameters for the reduction of 4-NP by Ag-Au@P(NIPAM-*co*-MAPTMS) before and after LCST.

Temperature	A(min^{-1})	E_a(J/mol)	ΔH(J/mol)	ΔS(J/mol·K)
Before LCST (25-30 °C)	27.23	1.25×10^4	0.97×10^4	-260.89
After LCST (35-40 °C)	321.93	1.80×10^4	1.39×10^4	-244.60

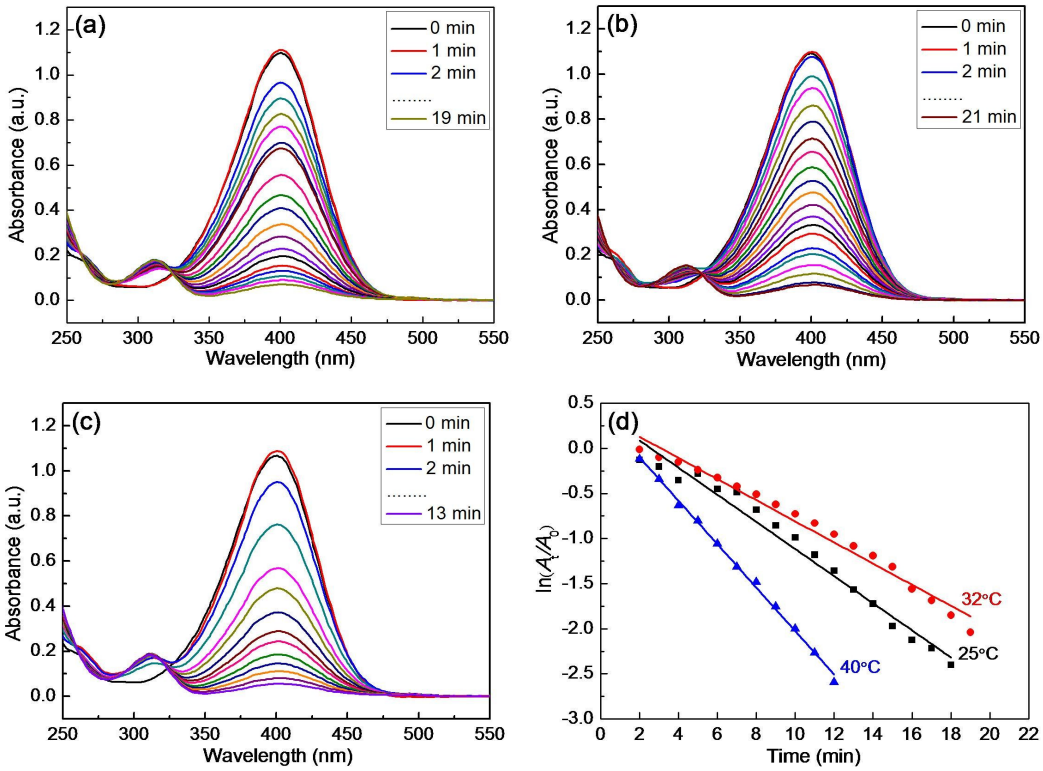

Fig. S7 UV-Vis absorption spectra and plots of the ln(A_t/A_0) versus time (d) for the reduction of 4-NP in the presence of Ag-Au@PNIPAM hybrid microgels under different temperature. (a) 25 °C, (b) 32 °C, (c) 40 °C

Table S3 Comparison of apparent rate constant and intrinsic rate constant of different catalytic systems for the reduction of 4-NP.

Catalysts	Amount of catalyst (μg/mL)	Size of NPs (nm)	Apparent rate constant (min^{-1})	Intrinsic rate constant (L/(min·g))	Refs.
Ag-P(NIPAM-*co*-AAm)	37180	15	0.2646 (32 °C)	0.0071	1
Ag-P(NIPAM-AAc-AAm)	66	20	0.883 (22 °C)	13.38	2
Ag-P(NIPAAm-HEMA-AAc)	56	10±3	0.916 (22 °C)	16.35	3
P(AAc)-Co	1000	-	0.0472 (30 °C)	0.0472	4
Ag@P(GSH)	219	6	1.02 (22 °C)	4.66	5
Ag@P(NIPAM-*co*-MAPTMS)	7.5	35±5	0.062 (25 °C)	8.27	This work
Ag-Au@P(NIPAM-*co*-MAPTMS)-3	7.5	35±5	0.174 (25 °C) 0.162 (32 °C)	23.2 21.6	This work

References

1 R. Begum, Z. H. Farooqi, E. Ahmed, K. Naseem, S. Ashraf, A. Sharif and R. Rehan, *Appl. Organometal. Chem.*, 2017, **31**, e3563.

2 R. Begum, K. Naseem, E. Ahmed, A. Sharif and Z. H. Farooqi, *Colloids and Surfaces A: Physicochem. Eng. Aspects*, 2016, **511**, 17-26.

3 R. Begum, Z. H. Farooqi, Z. Butt, Q. S. Wu, W. T. Wu and A. Irfan, *Journal of environmental sciences*, 2017, Doi: org/10.1016/j.jes.2017.12.003.

4 F. Bibi, M. Ajmal, F. Naseer, Z. H. Farooqi and M. Siddiq, *Int. J. Environ. Sci. Technol*, 2017, Doi: 10.1007/s13762-017-1446-4.

5 C. Kastner and A. F. Thünemann, *Langmuir*, 2016, **32**, 7383-7391.

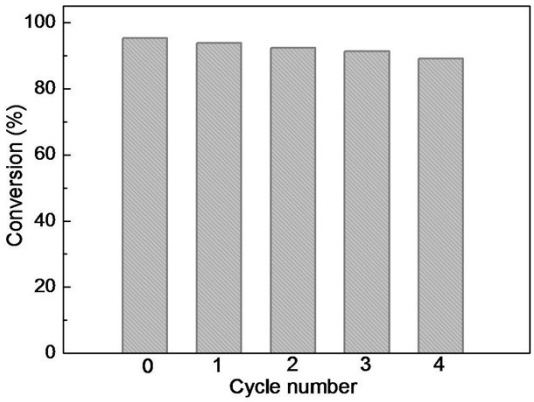

Fig. S8 Conversion of 4-NP in five successive cycles with Ag-Au@P(NIPAM-*co*-MAPTMS)-3 hybrid microgels.